AD-A053 393 WEIDLINGER ASSOCIATES NEW YORK F/G 8/7
TENSILE BEHAVIOR OF GEOLOGICAL MATERIAL IN GROUND SHOCK CALCULA--ETC(U)
MAR 77 J P WRIGHT, L WHITMAN DNA001-76-C-0127
UNCLASSIFIED DNA-4450T NL

| OF |
AD
A053393

END
DATE
FILMED
6-78
DDC

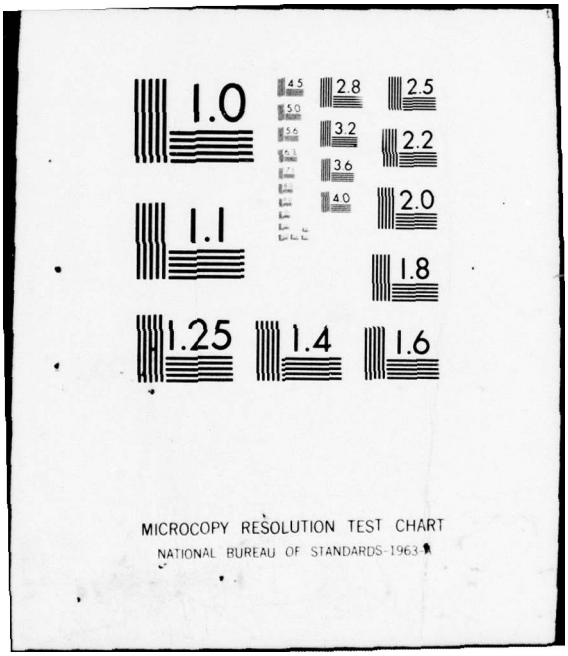
1.0
1.1
1.25
1.4
1.6
1.8
2.0
2.2
2.5
2.8
3.2
3.6
4.0
4.5
5.0
5.6
MICROCOPY RESOLUTION TEST CHART
NATIONAL BUREAU OF STANDARDS-1963-A

DNA 4450T

TENSILE BEHAVIOR OF GEOLOGICAL MATERIAL IN GROUND SHOCK CALCULATIONS, II

Weidlinger Associates
110 East 59th Street
New York, New York 10022

March 1977

Topical Report for Period January 1976—December 1976

CONTRACT No. DNA 001-76-C-0127

THIS WORK SPONSORED BY THE DEFENSE NUCLEAR AGENCY
UNDER RDT&E RMSS CODE B344076464 Y99QAXSB04901 H2590D.

Prepared for
Director
DEFENSE NUCLEAR AGENCY
Washington, D. C. 20305

Destroy this report when it is no longer needed. Do not return to sender.

UNCLASSIFIED

SECURITY CLASSIFICATION OF THIS PAGE *(When Data Entered)*

REPORT DOCUMENTATION PAGE

READ INSTRUCTIONS BEFORE COMPLETING FORM

1. REPORT NUMBER: DNA 4450T

2. GOVT ACCESSION NO.:

3. RECIPIENT'S CATALOG NUMBER:

4. TITLE *(and Subtitle)*: TENSILE BEHAVIOR OF GEOLOGICAL MATERIAL IN GROUND SHOCK CALCULATIONS, II.

5. TYPE OF REPORT & PERIOD COVERED: Topical Report, Jan 76—Dec 76,

6. PERFORMING ORG. REPORT NUMBER:

7. AUTHOR(s): Joseph P. Wright
Lorraine Whitman

8. CONTRACT OR GRANT NUMBER(s): DNA 001-76-C-0127

9. PERFORMING ORGANIZATION NAME AND ADDRESS:
Weidlinger Associates
110 East 59th Street
New York, New York 10022

10. PROGRAM ELEMENT, PROJECT, TASK AREA & WORK UNIT NUMBERS:
NWED Subtask
Y99QAXSB049-01
B049

11. CONTROLLING OFFICE NAME AND ADDRESS:
Director
Defense Nuclear Agency
Washington, D.C. 20305

12. REPORT DATE: March 1977

13. NUMBER OF PAGES: 48 (44 p.)

14. MONITORING AGENCY NAME & ADDRESS *(if different from Controlling Office)*: DNA, SBIE
4450T, AD-E300 179

15. SECURITY CLASS *(of this report)*: UNCLASSIFIED

15a. DECLASSIFICATION/DOWNGRADING SCHEDULE:

16. DISTRIBUTION STATEMENT *(of this Report)*

Approved for public release; distribution unlimited.

17. DISTRIBUTION STATEMENT *(of the abstract entered in Block 20, if different from Report)*

18. SUPPLEMENTARY NOTES

This work sponsored by the Defense Nuclear Agency under RDT&E RMSS Code B344076464 Y99QAXSB04901 H2590D.

19. KEY WORDS *(Continue on reverse side if necessary and identify by block number)*

Uniqueness
Stability
Rate Effects
Tension Models
Brittle Fracture
Geological Material
Ground Shock

such as those described in this report,

20. ABSTRACT *(Continue on reverse side if necessary and identify by block number)*

As part of a continuing study of material models for ground shock calculations, some aspects of both rate-dependent and rate-independent models for tensile behavior are examined. In particular, the SRI brittle fracture model is studied and compared with a simple tension cut off procedure. For large-scale problems ~~(described herein)~~, it is important to avoid rate-dependent brittle tensile models, if possible, since rate effects appear to be important only on time scales much smaller than are resolvable in dynamic calculations. On (over)

DD FORM 1 JAN 73 1473 EDITION OF 1 NOV 65 IS OBSOLETE

UNCLASSIFIED

SECURITY CLASSIFICATION OF THIS PAGE *(When Data Entered)*

373 050

JOB

(cont)

20. ABSTRACT (Continued)

the other hand, rate-independent brittle fracture models are incompatible with current continuum uniqueness-stability theory and hence may not be useable for these problems. It is necessary to examine this situation if tensile modeling techniques are to improve. Some ideas for resolving this conflict are discussed and recommendations for further study are made.

TABLE OF CONTENTS

I INTRODUCTION

In seeking to improve the tensile modeling of geological materials for use in ground shock applications, a review, Ref. [1], was made of current practices in the field. Both rate-dependent and rate-independent models were summarized and it was recommended that some of the more promising models be investigated in somewhat greater detail.

In this report, the Stanford Research Institute (SRI) brittle fracture model (rate-dependent) is studied and, to some extent, is compared with a simple tension cut-off procedure (rate-independent). Although the SRI model was originally designed for metals, it has been adapted for ground shock applications in rocks in recent years. A copy of the model routine BFRACT was obtained from SRI. It has been examined theoretically and computationally for one-dimensional problems and some of the results are presented herein. The model was first exercised to simulate simple uniaxial extension and then incorporated into the one-dimensional wave code WONDY for plate slap calculations.

As written, the BFRACT algorithm requires the storage of more than ten memory parameters per mesh point. This added computer storage requirement is a major impediment to its direct incorporation into large-scale ground shock calculatons. In Section II, modifications to the algorithm are suggested to ameliorate this situation, following a review of the continuum assumptions upon which BFRACT is based. In Section III, one-dimensional numerical tests of BFRACT, with and without modifications, are presented. It is shown that BFRACT is highly rate-dependent, but much less sensitive to the variation of many of the BFRACT material parameters.

In Section IV, it is pointed out that time steps greater than 100

microseconds are used in typical large-scale ground shock calculations, but that time scales of less than 10 microseconds are believed necessary to resolve the rate-dependent tensile behavior of geological materials. For practical computations, therefore, it is important to avoid rate-dependent models, if possible. On the other hand, it is pointed out that current continuum uniqueness-stability theory is incompatible with rate-independent brittle fracture models even though such models have been used in computations for many years. It is necessary to examine this situation further to resolve these inconsistencies. It may be possible to extend current uniqueness-stability theory to permit some form of stress discontinuity. Another possibility is that acceptable results may be obtainable, for some types of ground shock problems, if a plasticity model (such as contained in the cap model routine CAP75, Ref. [2]), is used to model tensile failure. These ideas and others can be examined by means of a series of one-dimensional wave code calculations coupled with some theoretical studies designed to focus on the question of which types of tensile models are appropriate for ground shock applications. Conclusions and recommendations, based on the above, are summarized in Section V.

II BRITTLE FRACTURE MODEL OF SRI

A. Introduction

Although the brittle fracture model of SRI was originally designed for metals, Refs. [3, 4, 5], it has been, more recently, adapted for ground shock applications in rocks, Refs. [6, 7, 8]. This model is based on rate-dependent concepts of fracture, including crack nucleation rates and crack growth rates. Stress-strain behavior of the material is postulated for various stages of damage, including full fragmentation, defined as coalescence of cracks and full separation.

A copy of the model routine, BFRACT, Ref. [5], was obtained and has been examined theoretically, as well as computationally, for one-dimensional problems. The basic postulates of the model and the results of numerical investigations are discussed in this section. Some modifications of BFRACT, based on the assumption of spatial isotropy, are suggested.

B. Constitutive Equations for Cracked Material

The BFRACT model routine contains many elements common to other constitutive equation routines and these assumptions are summarized below.

It is presumed that compressive states are represented by an appropriate set of stress-strain relations and that, at some point based on experimental data, the tensile behavior requires a representation of cracks and their propagation. The model is based on continuum concepts and thus it is assumed that the microscopic cracks can be represented by means of a few simple macroscopic parameters.

When fracture begins, the specific volume, V, at a point in the continuum is given by the sum

$$V = V_s + V_c \tag{1}$$

where V_s is the specific volume of the solid material, and V_c is the specific volume of the cracks. The pressure, P, at a point is assumed to be related to the pressure, P_s, of the solid material by the Carroll-Holt equation, Ref. [9], for porous materials, i.e.,

$$P\ V = P_s V_s \tag{2}$$

Since tensile strains associated with brittle fracture are initially small, a linearized Mie-Grüneisen equation of state is assumed for the solid behavior

$$P_s = K_o \left(\frac{V_o}{V_s} - 1\right) + \frac{\Gamma E}{V_s} \tag{3}$$

where K_o is the ambient bulk modulus, V_o the initial solid specific volume, Γ the Grüneisen ratio and E the internal energy. Internal energy changes are assumed independent of the "energy of distortion" so that

$$dE = -\ P\ dV \tag{4}$$

The deviatoric stress tensor, s_{ij}, at a point is calculated by means of

$$ds_{ij} = 2\ \mu_{red} \left(d\varepsilon_{ij} - \frac{1}{3}\ \delta_{ij}\ \frac{dV}{V}\right) + \theta_{ij} \tag{5}$$

where ε_{ij} is the strain tensor, δ_{ij} the Kronecker delta, θ_{ij} is a

correction due to rotation (large displacement theory) and μ_{red} is the reduced shear modulus*)

$$\mu_{red} = \mu_o \left(1 - 1.88 \frac{V_c}{V}\right) \tag{6}$$

The shear strength*), Y, is assumed to decrease linearly with increasing porosity or crack volume so that

$$Y = Y_o \left(1 - 4 \frac{V_c}{V}\right) \tag{7}$$

where a von Mises yield condition

$$\sqrt{J_2'} = Y/\sqrt{3} \tag{8}$$

is assumed and J_2' is the second invariant of the stress deviators.

It remains only to specify an equation for the specific volume of the cracks, V_c. For a general distribution of cracks one may write

$$V_c = \int_o^\infty v_c(R)\, dN_c(R) \tag{9}$$

where v_c is the volume of cracks with radius R, and dN_c is the number density of cracks with radius R. The Sneddon relationship for the elastic opening of a penny-shaped crack, Ref. [10], is assumed so that the ellipsoidal volume of the crack is

$$v_c = \frac{16\ (1 - \nu^2)}{3E} R^3 \sigma \tag{10}$$

---

*) The factors 1.88 and 4 in μ_{red} and Y are, in fact, material parameters, but were chosen as constants in all SRI work so far. See Ref.[4, p. 20] for discussion.

where ν is Poisson's ratio, E is Young's modulus, and σ is the tensile stress normal to the plane of the penny-shaped crack.

C. Nucleation and Growth Rates

The laws which govern the size distribution and growth rates of crack radii are the relations which distinguish the SRI model from other theories. A distribution function for the inherent flaws (penny-shaped cracks) in a brittle substance, as well as the laws governing their continued nucleation and growth under tensile stress, are postulated, with the SRI experimental program providing the material parameters.

The usual size distribution of penny-shaped cracks seen in brittle materials is an exponential form

$$N_c = N(t) \exp (- R/R_1) \tag{11}$$

where N_c is the number density of cracks with radii greater than R, N(t) is the total number density at time t, and R_1 is the shape parameter of the crack size distribution. The crack radius, R, is also a function of time which will subsequently be defined.

The rate at which new cracks nucleate under the influence of a tensile stress*) is taken to be

$$\dot{N} = \begin{cases} \dot{N}_o \exp \left[\dfrac{\sigma - \sigma_{no}}{\sigma_1}\right] , & \sigma < \sigma_{no} \\ 0 , & \sigma \geq \sigma_{no} \end{cases} \tag{12}$$

*) Stress is assumed positive in compression.

where $\dot{N}_o$ is the initial nucleation rate, σ_{no} is the nucleation stress threshold*) and σ_1 is the nucleation stress sensitivity parameter.

The crack growth law found to give best agreement with experimental data, even for brittle materials, is of a viscous form (see Ref. [11])

$$\dot{R} = \begin{cases} T_1 \, (\sigma - \sigma_{go}) \, R \quad , & \sigma < \sigma_{go} \\ \\ 0 \quad , & \sigma \geq \sigma_{go} \end{cases} \tag{13}$$

where T_1 is a constant related to the "viscosity" and σ_{go} is the growth threshold stress.

D. Full Fragmentation

Up to this point, it has been tacitly assumed that the growing cracks do not influence one another. To go from mild to severe damage, the coalescence of cracks and the resultant formation of fragments which cannot support tensile stresses must be accounted for. This is done through the following heuristic argument.

If it is assumed that the radius of a fragment, R_f, is proportional to the size, R, of the cracks forming it, and that the number density of possible fragments, N_f, is proportional to the number density of cracks, N_c, two material constants are defined

$$\gamma = \frac{R_f}{R} \tag{14}$$

*) The apparent discontinuity in the nucleation rate function is not significant since σ_{no} is taken to be the tensile stress at which the crack volume first becomes non-zero.

and

$$\beta \equiv \frac{N_f}{N_c} \tag{15}$$

Experience shows γ to be near one and β, reflecting fragment shape, to be one-quarter for eight-sided fragments, as are most often assumed. A third parameter, T_f, relating relative fragment volume, v_f, to radius, is also of order unity.

$$v_f = T_f \, R_f^3 \tag{16}$$

Then, the relative volume of all fragments is

$$V_f = \int v_f \, dN_f$$

Upon inserting Eqs. (14) - (16),

$$V_f = T_f \gamma^3 \, \beta \int R^3 \, dN_c \tag{17}$$

The number density of cracks with radius R, dN_c, is obtained from Eq. (11).

While the function V_f varies continuously from slightly cracked to fully fragmented material states, it is thought to overestimate fragmentation in the early stages of damage. It is likely that some threshold density of cracks must be reached before the likelihood of cracks intersecting sufficiently to form fragments becomes significant. This threshold value, V_*, defining the beginning of crack coalescence, is given in terms of the material constants discussed above and T_c, a measure of material brittleness, Refs. [5, 11]

$$V_* = \beta\gamma^3 \frac{T_f}{T_c} \tag{18}$$

The actual relative fragment volume, V_f^a, is defined then as

$$V_f^a = \frac{V_f - V_*}{1 - V_*} \quad , \quad V_f > V_*$$
$$= 0 \quad , \quad V_f \leq V_* \tag{19}$$

Total porosity, V_v, is the sum of the crack volumes determined from Eqs. (9) - (13) and the portion of the solid volume which has fragmented

$$V_v = V_c + V_f^a V_s \tag{20}$$

(The three quantities, V_v, V_c, V_s, are specific volumes. V_f^a is a relative volume).

E. BFRACT Algorithm

While the nucleation and growth laws are both given as functions of the normal stress, specifying this quantity for each propagating crack would be enormously cumbersome and some simplifying assumptions are made. The above continuum model is implemented in BFRACT by first assuming that each computational cell can be broken into an array of crack orientations or "bins", Ref. [4, p. 21]. For two-dimensional behavior, each bin is defined as containing cracks perpendicular to ϕ^i (in the x, y plane), and to ψ^i (perpendicular to the x, y plane), where the index, i, refers to the i-th bin. Then, direction-dependent damage functions are specified relative to these bin orientations. Thus, $\sigma^i_{\phi\psi}$ is the tensile stress in the direction (ϕ^i, ψ^i), R^i is the radius of a crack perpendicular to and growing under the influence of $\sigma^i_{\phi\psi}$, and dN_c^i is the time-dependent number density of cracks with radii equal to R^i.

It is useful to see the transition from continuum expression to algorithm for a specific function. Integrating Eq. (13) gives

$$R(t) = R(o) \exp \left[\int_o^t T_1 \left(\sigma (t') - \sigma_{go} \right) dt' \right] \tag{21}$$

for the radius of an arbitrary crack under the influence of tensile stress σ ($< \sigma_{go}$). If the time of observation is taken incrementally close to a time, t_o, at which the radius was known to be R_o, then

$$R(t) = R(t_o + \Delta t) \approx R_o \exp \left[T_1 \left(\bar{\sigma} - \sigma_{go} \right) \Delta t \right] \tag{22}$$

where $\bar{\sigma}$ is the average stress during the time interval Δt. Using the bin breakup,

$$R^i(t) \approx R_o{}^i \exp \left[T_1 \left(\bar{\sigma}^i_{\phi\psi} - \sigma_{go} \right) \Delta t \right] \tag{23}$$

Volumetric damage-related functions require summation over the bins in each cell. So, for example, the relative fragment volume, defined in Eq. (17), becomes

$$V_f = T_f \gamma^3 \beta \sum_i \int (R^i)^3 \, dN_c^i \tag{24}$$

F. Storage Requirements

One consequence of this partitioning into bins is the need to save at least "b" memory parameters per computational element, where b is the number of bins. In fact, two time-dependent functions, $N^i(t)$ and $R^i(t)$, must be stored for each bin. In addition, the void volume, V_v, and the unfragmented volume fraction, f_u, are stored, where

$$f_u = 1 - V_f{}^a$$

making a total of 2b + 2 memory parameters per element. As BFRACT is currently implemented, five bins per element are assumed, making a total of twelve items per element for the characterization of brittle tensile fracture.

G. Possible Modifications of BFRACT

The function of BFRACT is to calculate the time-dependent growth of damage caused by the application of tensile stress, while accounting for the strength reduction caused by the developing damage. The routine functions well for small-scale shock loading problems and has been used successfully to model plate slap experiments, Ref. [5], armor penetration problems, Ref. [5], and laboratory-dimension crater detonations, Ref. [8].

However, for large-scale applications, such as many ground shock problems, a scheme which requires more than ten memory parameters to model tensile behavior appears too costly. This seems especially true when the uncertainties in modeling the in situ material are considered. For this reason, it was decided to examine ways of simplifying BRFACT while retaining the nucleation, growth and fragmentation concepts. The hope is that a significant portion of the modeling capability can be preserved but at a more modest cost in computer storage.

Two approaches toward simplification could be considered, depending on the type of fracture occurring. In the case of brittle fracture (e.g. of rocks), cracking tends to be highly localized and oriented normal to the axis of maximum principal stress. In contrast, ductile fracture (e.g. of many soils or metals) occurs in a form which is characterized by spherical voids and hence is associated with spatial isotropy.

Thus, for brittle fracture, the use of the maximum tensile stress in place of $\sigma_{\phi\psi}$ would seem appropriate. The maximum principal stress criterion, if implemented without the use of bins, should lead to a significant reduction in storage requirements. Similarly, for ductile

fracture, the use of a combination of stress invariants (e.g. the pressure and J_2') in place of $\sigma_{\phi\psi}$ would seem appropriate and, if implemented without bins, should lead to a reduction in storage requirements.

In fact, as the continuum concepts underlying BFRACT have actually been implemented in difference form by SRI, $\sigma_{\phi\psi}$ is variously approximated, depending on its sensitivity in a calculation and upon the brittle material itself. In some expressions it is taken as a function of the solid pressure, in others as some linear combination of the solid pressure and the most tensile stress deviator. Thus, examining different approximations for $\sigma_{\phi\psi}$, in the search for a more economical BFRACT, seems quite appropriate.

III ONE-DIMENSIONAL STUDIES OF BFRACT

A. Introduction

In the preceding section, the basic continuum relations underlying the model routine BFRACT were reviewed, and some possible modifications of the algorithm were discussed. In this section, the results of some simple one-dimensional calculations with BFRACT are presented, and the feasibility of some of the modifications is tested. At the same time, the rate-dependence of the model routine, and its sensitivity to parameter changes, is explored.

B. Armco Iron

The material chosen for the studies is Armco iron, a well characterized brittle metal for which the SRI experimental program has provided a full set of model parameters. The reason for this is that geological materials, which are the main concern of the present study, have been investigated less fully and are more complex. In Table 1, some general properties of Armco iron are listed. In Table 2, those parameters necessary for the implementation of BFRACT are given.

Table 1. Material Properties of Armco Iron (From Ref. [5])

Mass density, ρ_o	7.85 gm/cm^3
Poisson's ratio, ν	0.2801
Grüneisen parameter, Γ_o	1.690
Bulk modulus, K_o	1.589×10^{12} dyn/cm^2
Shear modulus, μ_o	8.190×10^{11} dyn/cm^2
Initial yield strength, Y_o	5.50×10^{9} dyn/cm^2
Bulk sound speed, c_o	4.499×10^{5} cm/sec

Table 2. Fracture*) and Estimated Fragmentation**) Parameters for Armco Iron

Code Name	Name In Derivation	Parameter Definition	Value	Units
TSR(1)	T_1	Growth coefficient	-6.0×10^{-4}	$cm^2/dyn/sec$
TSR(2)	σ_{go}	Growth threshold	-2.0×10^{8}	dyn/cm^2
TSR(3)	R_1	Nucleation crack size distribution	5.0×10^{-5}	cm
TSR(4)	$\dot{N}_o$	Nucleation rate coefficient	4.6×10^{12}	$No./cm^3/sec$
TSR(5)	σ_{no}	Nucleation threshold stress	-3.0×10^{9}	dyn/cm^2
TSR(6)	σ_1	Nucleation stress sensitivity	-4.56×10^{9}	dyn/cm^2
TSR(10)	β	Ratio of the number of fragments to the number of cracks	0.25	---
TSR(11)	γ	Ratio of fragment radius to crack radius	1.0	---
TSR(12)	V_*	Threshold relative volume of potential fragments to produce actual fragments	0.2	---
TSR(13)	T_f	Coefficient relating fragment shape to fragment volume	1.0	---

*) From Ref. [4, p. 57]

**) Based on values chosen for armor steel, Ref. [5, p. 89]

C. Uniaxial Extension Tests

The model routine BFRACT was driven in simple uniaxial extension at a constant strain-rate of 1.8×10^5 sec^{-1}. Fig. 1 shows a plot of tensile stress versus specific volume for Armco iron. The curve labeled "SRI" appeared in Ref. [5, p. 55], and the curve labeled "WA" was produced at Weidlinger Associates with BFRACT, using the parameters shown in Tables 1 and 2. The discrepancy of a few percent between the two curves is the result of using somewhat different parameter values (due in part to rounded values given in reports). Since the model is quite rate-sensitive (see below), a few percent difference is not surprising.

C.1 Stress Modifications of BFRACT

As a test of the hypothesis that, for ground shock purposes, BFRACT may be simplified without sacrificing significant modeling capability, the uniaxial extension test was rerun with the following modifications:

Option 1 - Pressure only

Option 2 - Three "bins" instead of five

In option 1, the quantity, $\sigma_{\phi\psi}$, which controls the development of tension-induced fragmentation, was taken to be independent of the (most tensile) deviatoric stress. Since in the present example the deviatoric stresses are an order of magnitude smaller than the pressure, it is to be expected that setting the shear modulus to zero in tension will not affect the results by more than about ten per cent.

In option 2, the number of bins per element was reduced from five to three (the minimum number which can be accommodated without recoding or suppressing a stress component). It is expected that this variation

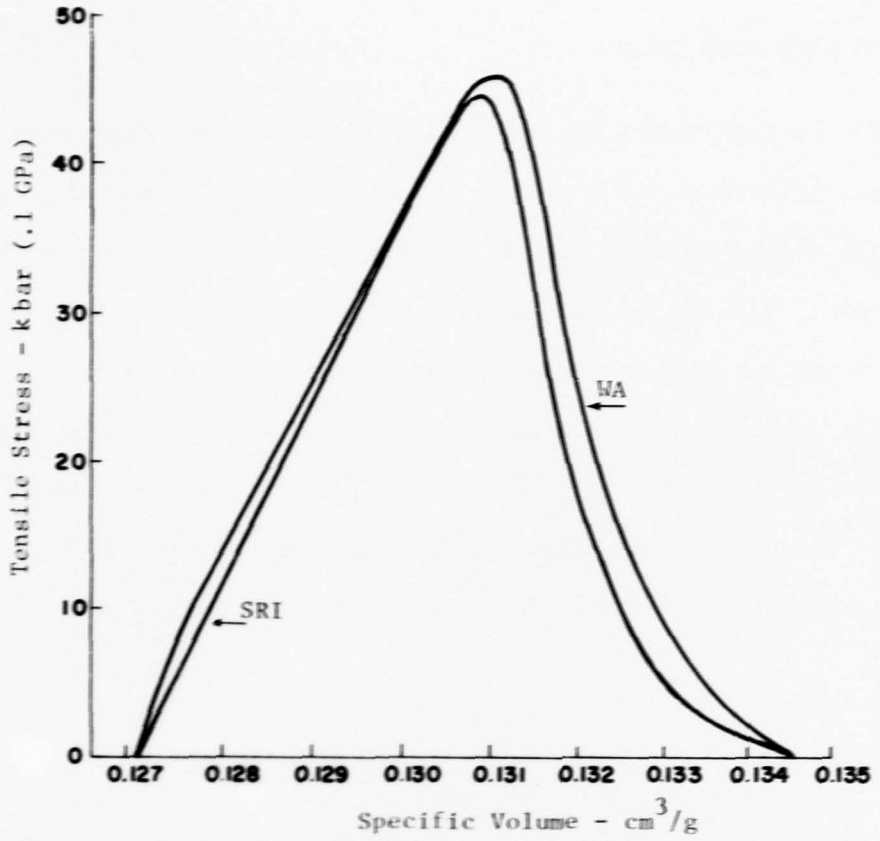

FIG. 1 STRESS-VOLUME PATH FOR CONSTANT STRAIN-RATE LOADING OF ARMCO IRON TO FRAGMENTATION

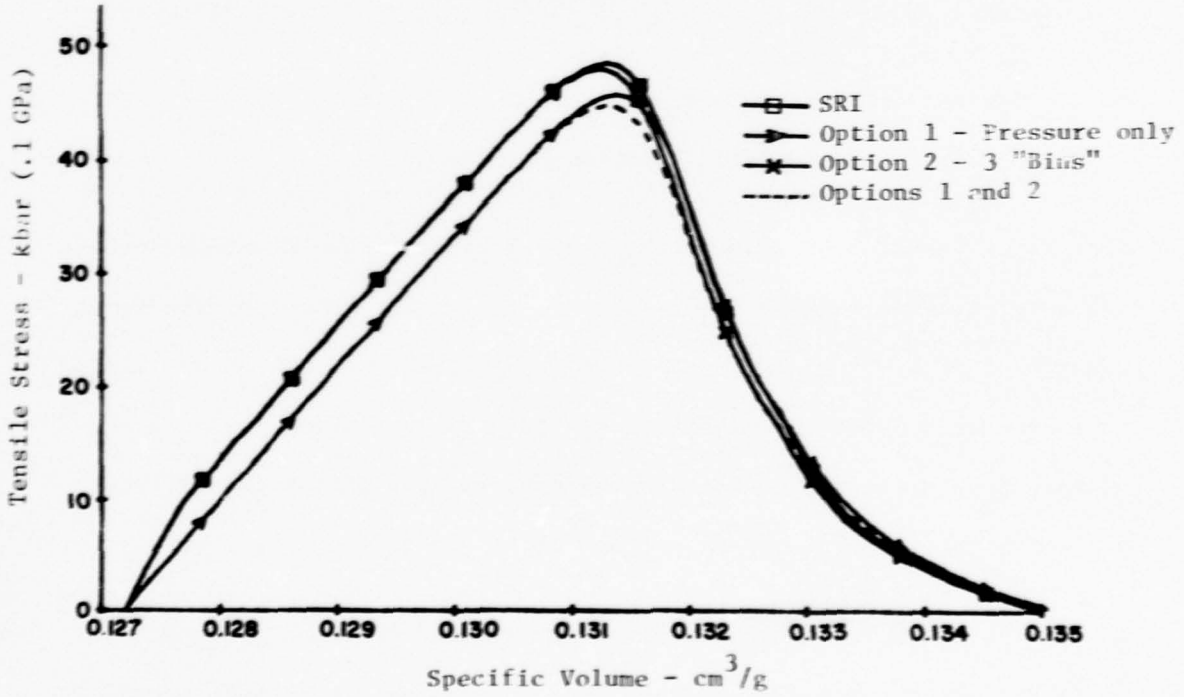

FIG. 2 UNIAXIAL EXTENSION TEST OF ARMCO IRON USING BFRACT AND STRESS MODIFIED OPTIONS OF BFRACT

will produce little change in the results of the present example.

Fig. 2 confirms these expectations. The curve labeled SRI is the same as that labeled WA in Fig. 1. The three other curves correspond to option 1, option 2, and options 1 and 2 combined. The distinguishable quantity, total strain to full fragmentation, is identical to within four significant figures, while peak stresses vary by less than ten per cent.

C.2 Rate-Dependence of BFRACT

BFRACT is a rate-dependent model devised for shock loading applications and the relationship between strain-rate and damage is highly nonlinear. For illustrative purposes, the strain-rate in the uniaxial extension problem under discussion was varied over several orders of magnitude. Total strains to full fragmentation and peak tensile stresses are listed in Table 3 and their variations confirm that BFRACT is strongly rate-dependent.

Table 3. Rate-Dependence of BFRACT (Uniaxial Extension)

Strain-Rate (sec^{-1})	Total Strain (%)	Peak Stress (kbars)*
1.8×10^{5}	6	- 48
1.8×10^{4}	2	- 19
1.8×10^{3}	< 1	- 8

*1 kbar = .1 GPa

As is well known, many metals exhibit ductile behavior (prior to fracturing in a brittle mode) under quasi-static testing conditions, as illustrated in Fig. 3, Ref. [3]. BFRACT is designed to model brittle behavior at high strain rates, but not the ductile transition expected in the quasi-static regime ($\dot{\varepsilon} \lesssim 10^{-3}$ sec^{-1}). The stress-strain curves of the three rapid extension tests are superimposed on Fig. 3 to facilitate

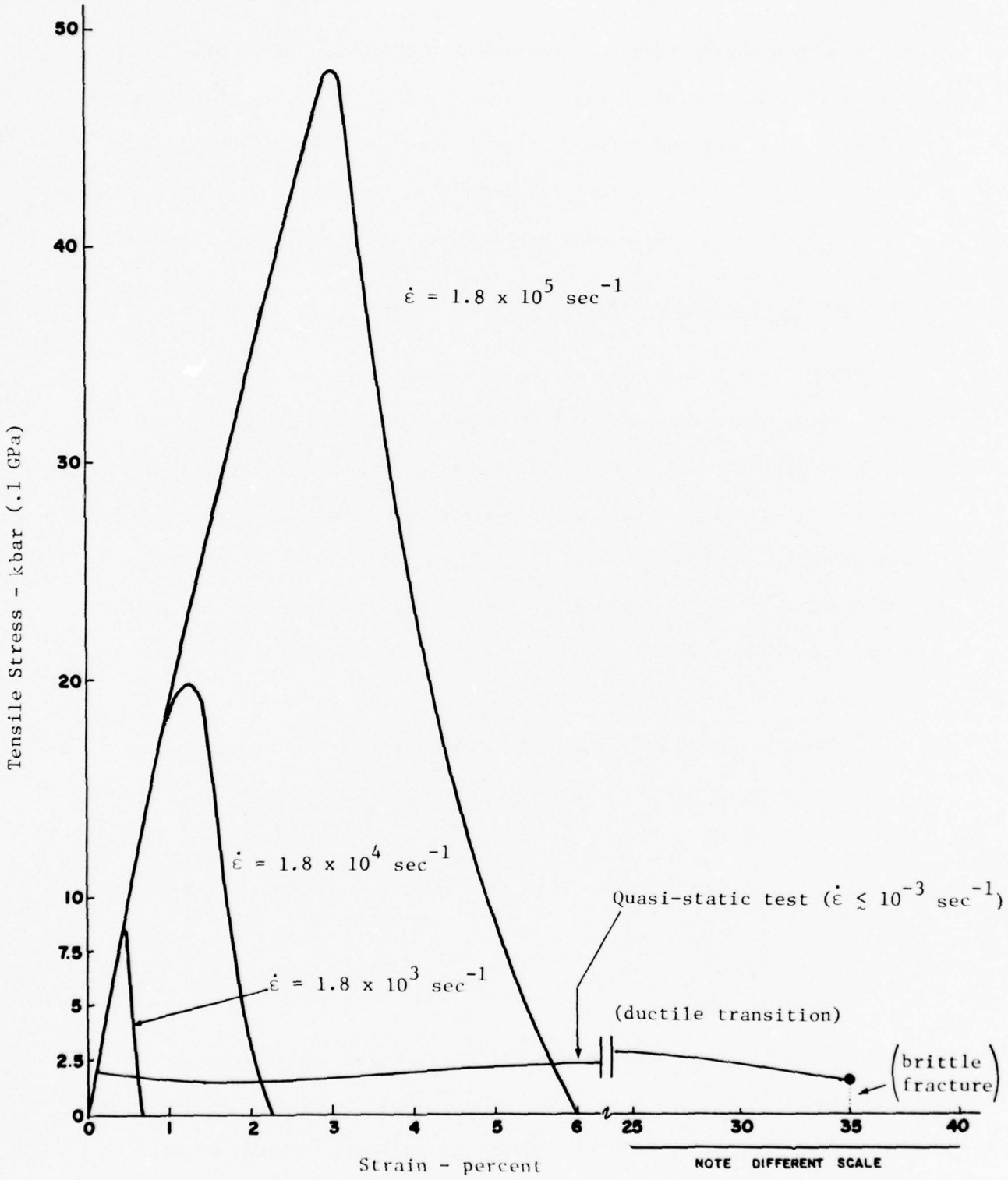

FIG. 3 RATE DEPENDENCE OF BFRACT FOR UNIAXIAL EXTENSION OF ARMCO IRON

comparison. Again, the strong rate-sensitivity of BFRACT is illustrated by the dramatic increase in peak tensile stress with strain-rate.

One of the potential dangers of adopting a model such as BFRACT without careful examination is that parameters may have been determined from a set of experiments with a limited range of strain-rates. If the routine is used indiscriminately for applications (and strain-rates) other than those for which it was envisioned, difficulties may arise. In fact, the use of a rate-dependent model adds another dimension to the modeling problem and should only be used if it is clearly necessary. An attempt to clarify this point is made in section IV.

D. Wave Code Calculations

The one-dimensional Lagrangian wave code WONDY (developed at Sandia) was selected as a convenient program by which BFRACT could be examined in dynamic calculations. The coding and data structure of WONDY allow for the inclusion of special equation of state and material model routines with a minimum of effort. The incompatibilities which arise between BFRACT and WONDY are easily overcome for the present purposes.

For comparative purposes, tensile behavior was modeled in three ways:

Case 1) BFRACT

Case 2) BFRACT with modification option 1 (MOD1)

Case 3) Instantaneous tensile fragmentation, i.e. the stress instantaneously reset to zero when the tensile strength of a material is exceeded

Case 3) represents one of the standard tensile fracture options available in WONDY, Ref. [12]. When the stress at a cell boundary is reset to zero, at the moment of fracture, the two free surfaces created are accommodated by the introduction of an additional node.

E. SRI Plate Slap Calculations

In the 1973 SRI report, Ref. [5], results of a tapered flyer plate experiment - copper impacting steel armor - were given and compared to two-dimensional code calculations in order to test the predictive capability of BFRACT. The experimental configuration is reproduced, from Ref. [5, p. 60], as Fig. 4.

For the coarse computational grid initially selected, the stress history near the end of the target was severely eroded and a clear spall signal was not evident. Therefore, the calculation was repeated with a finer grid in a one-dimensional calculation in which only the central region of the target and flyer were simulated. The discrepancy between measured and computed stress histories at the free surface of the target is shown in Fig. 5, Ref. [5, p. 64]. It was felt that agreement between the two waveforms might be improved by altering the material parameters in such a way as to delay the damage process. In particular, it was suggested, Ref. [5, p. 65], that the spall arrival time might be critically dependent on V_*, the threshold volume (relative) for fragmentation. This hypothesis was not tested for armor steel, but such parameter sensitivity was examined for Armco iron, as described in the next section.

F. Plate Slap Parameter Sensitivity Study

In the performance of the parameter sensitivity study, it would have

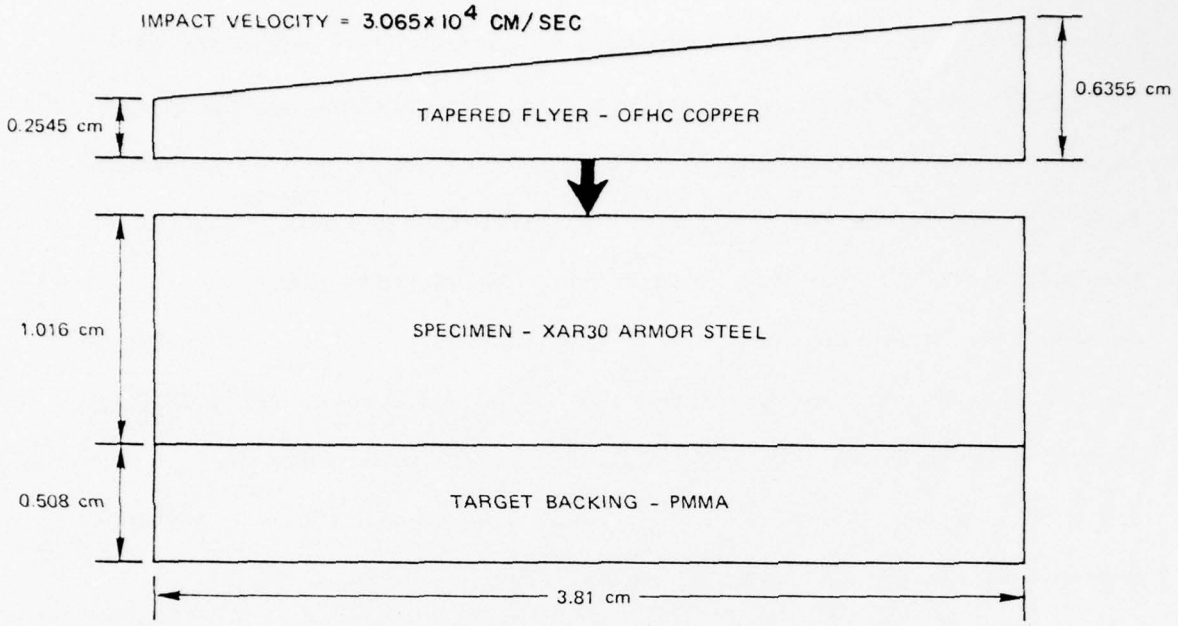

FIG. 4 CONFIGURATION FOR THE TWO-DIMENSIONAL SIMULATION OF FRAGMENTATION IN A TAPERED-FLYER IMPACT, Ref. [5, p. 60]

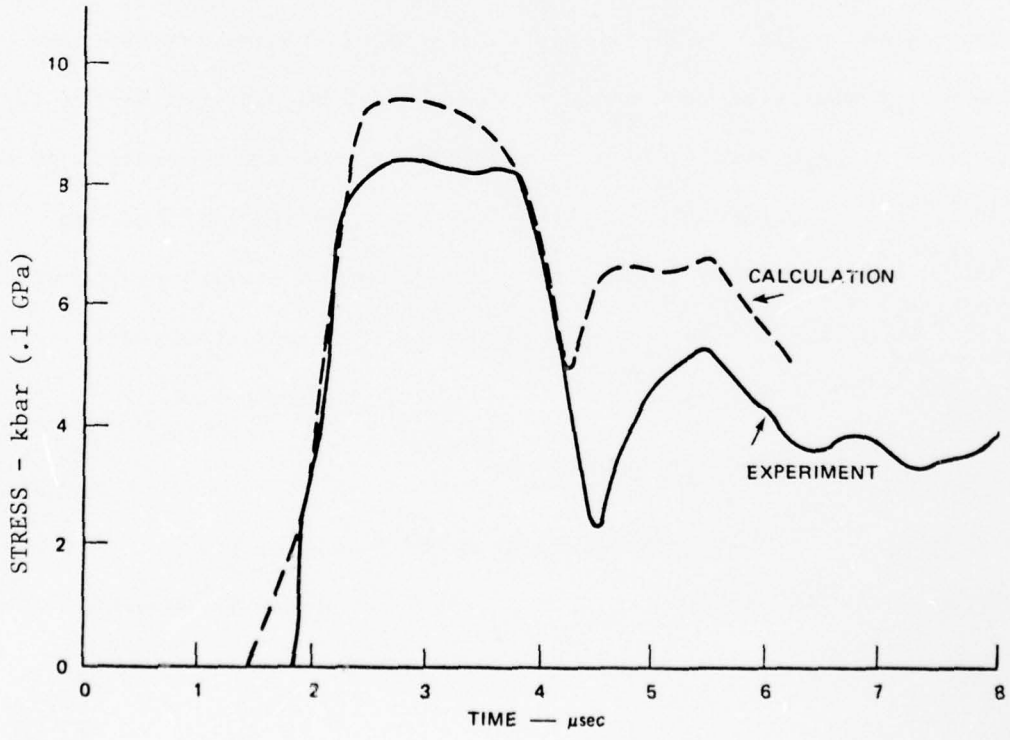

FIG. 5 COMPARISON OF MEASURED AND COMPUTED STRESS HISTORIES BEHIND XAR30 TARGET IN TAPERED-FLYER IMPACT, Ref. [5, p. 64]

been useful, for comparative purposes, to have utilized the plate slap configuration of Fig. 4. However, the BFRACT parameters appropriate to copper were not directly available (though they could have been obtained from SRI) and copper and steel are less rock-like in their responses to tension than the highly brittle Armco iron previously selected for examination. Thus, one-dimensional wave code calculations were made, as part of the present study, for the case of an Armco flyer (of 0.1270 cm) impacting on an Armco target (of 0.4233 cm) with a velocity of 5.0×10^4 cm/sec. The size and time scales are similar to the SRI one-dimensional simulation discussed in the previous section.

The free surface velocity histories of the Armco target are shown in Fig. 6 for the three cases of tensile modeling listed in Section D. For this simple problem, the first two cases - BFRACT and BFRACT MOD1 - are practically indistinguishable. As expected, instantaneous fragmentation results in a slightly earlier spall signal arrival time. The velocity histories subsequent to the spall time are similar but the instantaneous case results in a slightly higher average velocity. This is probably due to the fact that free surface velocity continues to decrease, once the loading wave reflects, until the arrival of the spall signal. Thus, the earlier the time of spall, the less the velocity has decreased.

The sensitivity of BFRACT to rate-dependence was discussed earlier and is quite strong, as shown in Table 3 and Fig. 3. In order to study material parameter sensitivity, the parameter list can be separated into a fracture set:

$$[TSR(J),\ J = 1,\ 6]$$

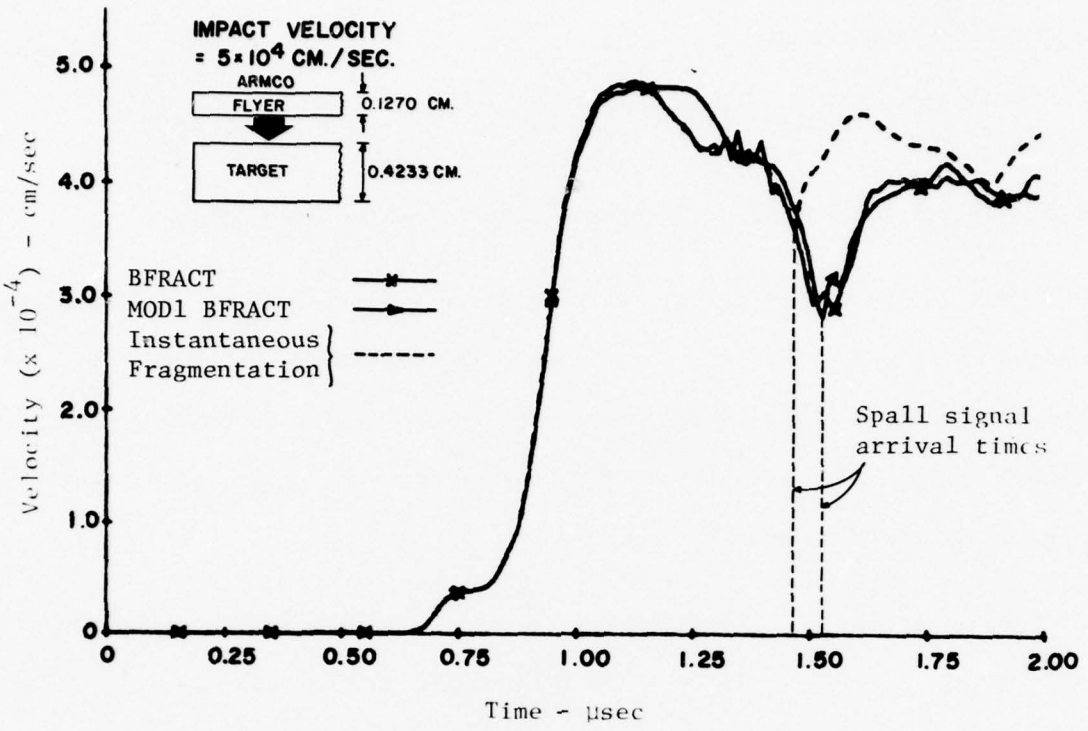

FIG. 6 COMPARISON OF COMPUTED FREE SURFACE VELOCITY HISTORIES OF ARMCO TARGET FOR THREE CASES OF TENSILE MODELING

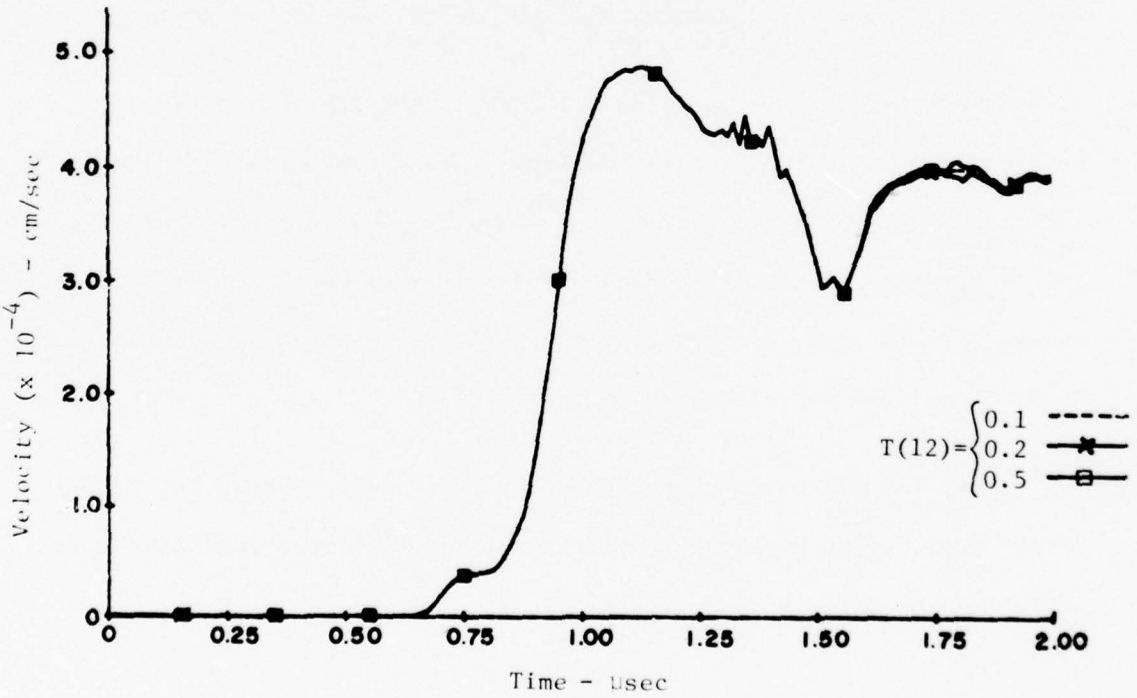

FIG. 7 COMPARISON OF COMPUTED FREE SURFACE VELOCITY HISTORIES OF ARMCO TARGET FOR DIFFERING VALUES OF PARAMETER T(12)

and a fragmentation set:

[TSR(J), J = 10, 13]

(See Table 2 for the physical significance of these parameters.)

The value of V_*, [T(12)], was varied from 0.1 to 0.5, the original choice being 0.2. The free surface velocity histories are shown in Fig. 7 for these three values of V_*. No change was detected in spall signal arrival time and virtually no change occurred in the post-spall signal, contrary to expectations.

In an effort to detect sensitivity to the fragmentation parameter T_f, [T(13)] was increased from 1.0 to 4.0 (the latter being an alternate choice in various SRI BFRACT calculations.) The post-spall velocity history, shown in Fig. 8, became slightly oscillatory but the difference is not considered significant in the context of ground shock.

As another test of sensitivity, some of the fracture parameters were varied dramatically, being assigned values appropriate to armor steel rather than to Armco iron. As shown in Table 4, parameter values changed by as much as four orders of magnitude. While the spall signal arrival time, from Fig. 9, became less clearly defined, the post-spall signal was not altered very much.

Thus, the picture that emerges from this limited study is of the BFRACT model being highly rate-sensitive, but much less sensitive to a number of the material parameters.

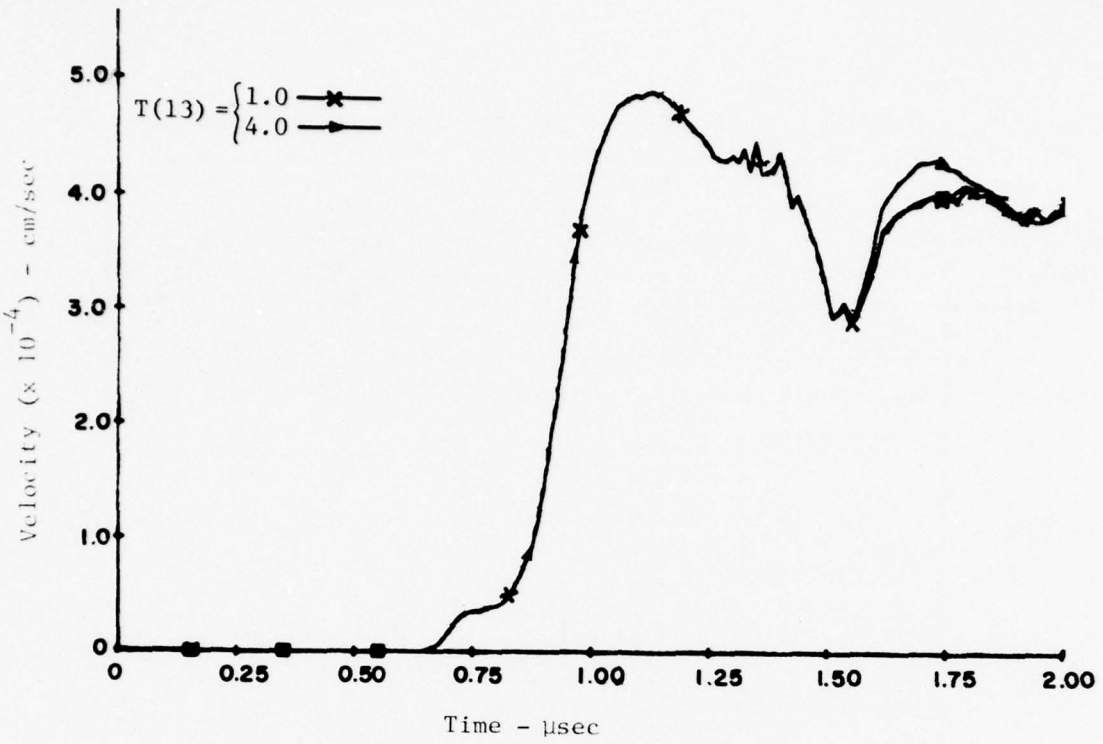

FIG. 8 COMPARISON OF COMPUTED FREE SURFACE VELOCITY HISTORIES OF ARMCO TARGET FOR DIFFERING VALUES OF PARAMETER T(13)

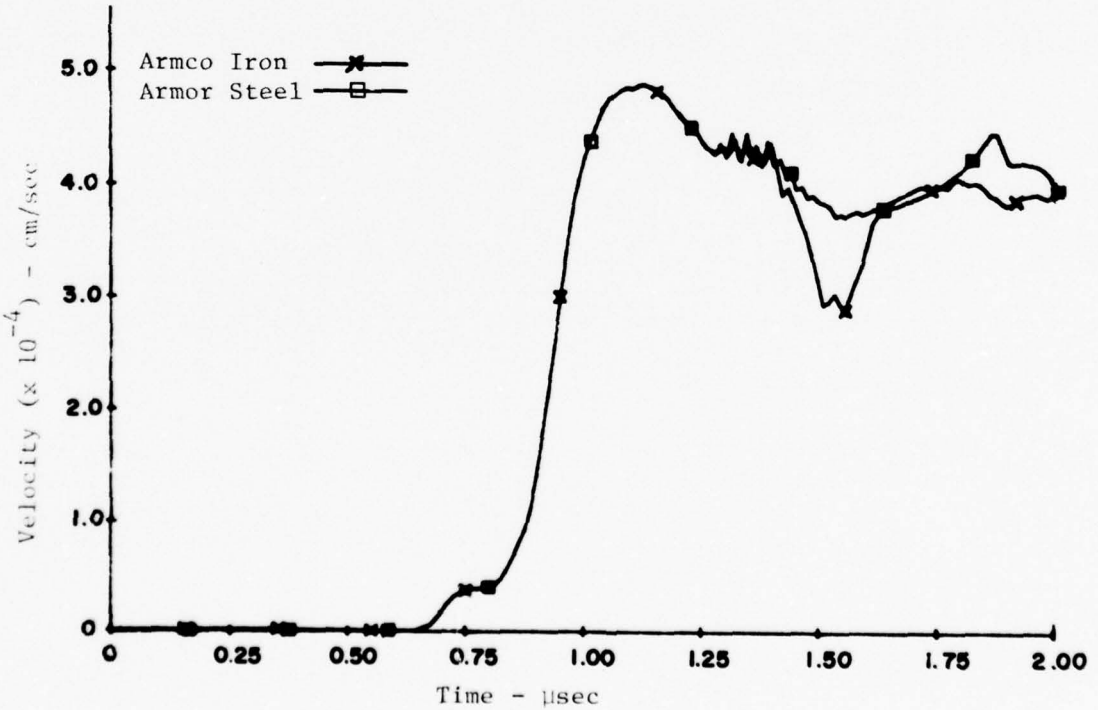

FIG. 9 COMPARISON OF COMPUTED FREE SURFACE VELOCITY HISTORIES OF ARMCO TARGET FOR TWO SETS OF FRACTURE PARAMETERS T(1) - T(6)

Table 4. Dynamic Fracture Parameters for Armor Steel*) and Armco Iron

Code Designation	Name In Derivations	Units	Armor Steel	Armco Iron
TSR(1)	T_1, Growth coefficient	$cm^2/dyn/sec$	-0.00012	-0.0006
TSR(2)	σ_{go} or P_{go}, Growth threshold	dyn/cm^2	0.0	-2.0×10^8
TSR(3)	R_1, Nucleation size parameter	cm	4.0×10^{-3}	5.0×10^{-5}
TSR(4)	$\dot{N}_o$, Threshold nucleation rate	$No.cm^3/sec$	5.0×10^8	4.6×10^{12}
TSR(5)	σ_{no} or P_{no}, Nucleation threshold	dyn/cm^2	-1.12×10^{10}	-3.0×10^9
TSR(6)	σ_1 or P_1, Nucleation sensitivity	dyn/cm	-7.4×10^8	-4.56×10^9

*) From Ref. [5, p. 89]

IV RATE-INDEPENDENT MODELS FOR GROUND SHOCK CALCULATIONS

A. Introduction

In the two preceding sections a rate-dependent model, based on experimental tests, has been examined in some detail as a candidate model for tensile behavior of geological materials in ground shock calculations. It is important at this point to try to specify, as clearly as possible, the type and scale of problems which are intended by the phrase "ground shock applications." This is done in the present section and it is argued that, for practical reasons, tensile behavior should be modeled as a rate-independent effect for this class of problems.

B. Large-Scale Ground Shock Problems

There are many land-based, near surface, defensive systems for which ground motion effects from large-scale explosions are of concern (see Fig. 10). Such systems would not be expected to survive a one megaton nuclear surface burst at a distance of less than, say, 200 meters because this distance is less than the crater radius in ordinary geologies. However, beyond two or three crater radii, it is possible to design protective structures, if the expected airblast and ground shock effects can be assessed. It is a currently accepted principle that the cost of such systems are kept to a more reasonable level if site-specific, threat-specific case studies are made. In order to reduce the number of case studies to a tolerable level, an attempt must be made to characterize the most critical parameters for such problems.

The threat-specific parameters are, from the standpoint of ground shock, relatively few in number compared to the site-specific parameters. For many applications, the size and location of the explosion are all

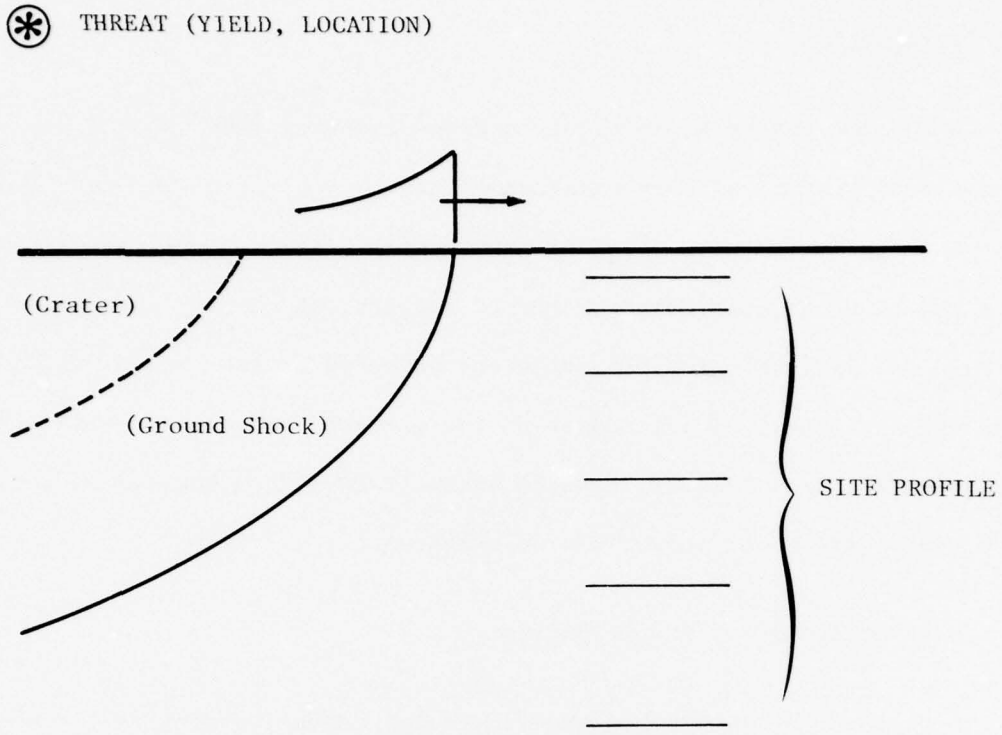

TYPICAL RANGES OF INTEREST (1 MT): 0.3 to 3 kilometers

TYPICAL TIMES OF INTEREST (1 MT) : 0.1 to 10 seconds

FIG. 10 LARGE-SCALE GROUND SHOCK PROBLEMS

that are required. (Other, roughly equivalent, parameters are also used.) Given these parameters, it is presumed that an air overpressure time history which is independent of azimuthal direction can be defined and used as an applied surface loading. This procedure has many hidden assumptions such as:

a) details of the explosive process are not important,

b) details of crater formation are not important,

c) details of air-ground interactions are not important.

The site-specific parameters are usually characterized by a site profile, which is a list of geological materials versus depth from ground surface. Implicit in this procedure are hidden assumptions such as:

a) the site can be considered to be horizontally layered,

b) each layer is homogeneous and isotropic (perhaps, transversely),

c) a material model for each layer can be determined.

Typically, with current continuum mechanics assumptions, the number of materials is between two and twelve, and the number of model parameters for each material is three or more. Thus, the number of model parameters needed to define a typical ground shock calculation is between six and a few hundred. If the assumption of horizontal layering is considered invalid or the models are made quite complicated, then the number of parameters can increase even further. Such complicated calculations are sometimes made for research purposes but should be avoided unless shown to be absolutely necessary since the effort, both experimentally and computationally, also will increase considerably. Since the introduction of rate-dependence will add a new dimension to the modeling process, it is worthwhile avoiding it, if possible, in ground shock applications.

C. Time Scales

The time scale associated with the rate-dependent tensile behavior of Armco iron can be estimated by studying the results of Sections II and III. Fig. 4 shows that the spall signal arrival times for the instantaneous and rate-dependent models differ by approximately 0.1 microseconds. The behavior of the iron in this problem can be described as follows. The flyer plate, impacting at a speed of 5×10^4 cm/sec, induces a compressive stress pulse with an amplitude of more than 90 kbars (9 GPa) in the iron. The stress pulse travels to the free end of the target, attenuating to about 60 kbars (6 GPa), reflects as a tensile wave, and creates tensile stresses (locally) of about 50 kbars (5 GPa). These tensile stresses can be sustained for only a short time however. As shown in Table 2 (Section III), for uniaxial extension, a peak tensile stress of 48 kbars (4.8 GPa) corresponds to a strain-rate $\dot{\varepsilon} = 1.8 \times 10^5$ sec^{-1}, and a total fragmentation strain $\varepsilon_f = 0.06$. At this strain-rate, the target will fragment in a time

$$t_f = \frac{\varepsilon_f}{\dot{\varepsilon}} = 0.33 \times 10^{-6} \text{ sec.}$$

Thus, the stress can be expected to reach its most tensile value of 50 kbars (5 GPa) in about half this time and then relax back to zero (see Fig. 1). It is quite reasonable then that the strain-rate effect leads to a difference of 0.1 microseconds in spall signal arrival times.

Using this case as a guide, it can be seen that a flyer plate of lower velocity will induce a lower strain-rate and the time delay will increase somewhat. (This trend has been observed by performing calculations with flyer plate speeds of 2.5×10^4 cm/sec and 1×10^4 cm/sec.) However, since the total fragmentation strain also decreases, the delay times do not change as rapidly as the strain-rate.

For example, if the induced tensile stress is about 8 kbars (.8 GPa) Table 2 shows that the fragmentation time, as estimated above, will be about 5 microseconds, and therefore a spall signal delay of 2 or 3 microseconds, as compared to instantaneous fracture, would be expected. Delay times much longer than a few microseconds are not detectable since the nucleation threshold, σ_{no}, is about 3 kbars (.3 GPa).

Up to this point, only Armco iron was examined because, as noted earlier, there is relatively little rate-dependent data available on geological materials. Nonetheless, it is possible to make some general statements about soils and rocks for use in ground shock problems. As indicated in Ref. [1], soils close to the surface have tensile strengths which are practically zero (less than 1 bar) while competent rocks at depth may have tensile strengths of more than 300 bars (.03 GPa). Compressive strengths are about 10 times the tensile strength, and modulus values are 100 to 1,000 tmes the compressive strengths. Table 5 shows representative values for several geological materials. (See, for example, Refs. [13, 14]).

Table 5 "Representative" Properties of Geological Materials

Material	Tensile Strength (kbar)*	Compressive Strength (kbar)	Loading Modulus (kbar)
"Soil"	.0001 to .001	.001 to .01	.3 to 3
Sandstone	.01	.1	30
Shale	.03	.3	100
Limestone	.1	1	300
Slate	.1	1	300
Granite	.2	1.5	500

*kbar = .1 GPa

These properties can vary considerably and are presented only as a rough indication of parameter values for some "typical" materials.

Data on rate-dependent tensile behavior of soils and rocks is quite meager but what little there is indicates that these materials do not require rate-dependent representation in large-scale ground shock calculations of the type depicted in Fig. 10. This is indicated by the fact that time scales of less than 10 microseconds are needed to resolve rate-dependence in these materials, yet ground shock calculations are conducted with time steps one or two orders of magnitude larger. The time step is controlled by wave propagation effects in a grid with boxes of the order of one meter or more and with wave speeds of six kilometers per second or less. Time steps greater than 100 microseconds are thus typical in large-scale ground shock applications. (On the other hand, small-scale problems, e.g. laboratory specimens of a few centimeters, require microsecond scale time steps and rate-dependent effects are detectable.)

D. Stability and Uniqueness

In view of the above time-scale discussion, it would be preferable to model tensile failure by means of a rate-independent continuum description. However, it is important that certain theoretical conditions be satisfied to guarantee that the continuum model yield a unique solution. To do so may require some modeling approximations which then need examination to determine their range of validity.

The key point to observe is that tensile failure is always associated with a phenomenon which can be characterized as brittle. There may be various ductile-like transitions but ultimately there appears a rapid relaxation from a measurable non-zero stress level to a zero stress. This

relaxation occurs in a time frame which is practically instantaneous. At this point, separation of the material occurs and it is no longer a true "continuum". However, in light of the variability of geological materials, it is unreasonable to try to keep track of the various particles which are created by this process.

On the other hand, the stability-uniqueness theory for rate-independent continua is incompatible with the instantaneous stress jumps (discontinuities) needed to represent brittle tensile failure*). One approach to this situation is to examine the uniqueness theory and try to extend the theory somewhat to permit these discontinuities. This is precisely what was done in the case of shock waves in continua, Ref. [15, p. 490]. Shock waves are stress jumps in compression (or shear) and can be understood physically as the limit of viscous material behavior as the viscosity becomes extremely small. Mathematically these discontinuous functions, called weak solutions, are obtained as the limit of continuous solutions. Numerically the solutions are discrete functions which approximate the weak solutions; viscosity is sometimes included in the scheme in order to maintain numerical stability. For linear equations the theory is complete, and for nonlinear problems a number of special cases (mainly one-dimensional) have been worked out completely so that a physically, mathematically and numerically coherent theory exists for a large class of problems. However, brittle tensile failure is quite different from a shock wave, and the theory referred to cannot simply be transferred to this situation.

---

*) Private communication, I.S. Sandler, Weidlinger Associates, 1976.

It is interesting then that numerical solutions have been obtained using models which represent idealized brittle failure. For example, the TENSOR code, Ref. [16, p. 198], has allowed a brittle fracture option for many years and (presumably) no instability has been traced to the use of this model. As another example, Ref. [17] presents results for one-dimensional spherical wave propagation in a material which is linearly elastic, except that an instantaneous brittle fracture model*) is introduced when a specified tensile hoop stress develops. There is no theoretical basis for accepting the results, but since they appear physically sensible and numerically stable there may be a mathematical basis for using certain types of brittle fracture models. One possibility then is to examine this numerical model to see whether the solution corresponds to a mathematically well-posed problem which is physically acceptable.

Another approach to the uniqueness problem is to try to model brittle failure by means of plasticity for which there is an established uniqueness theory. The hope here is that this approximation (i.e. ductile failure instead of brittle) can be shown to be acceptable for use in large-scale ground shock applications. This is the technique which is used in the current cap model routine, Ref. [2]. A series of simple one-dimensional calculations can be made which will allow this modeling technique to be examined. The stability and uniqueness theory for brittle fracture can be studied at the same time quite conveniently and recommendations concerning these ideas are discussed in Section V.

*) The brittle fracture model in TENSOR reduces to the model used in Ref. [15] for the case of spherical symmetry.

V CONCLUSION

A. Summary

As recommended in Ref. [1], the SRI rate-dependent brittle fracture model (as implemented in BFRACT) has been examined by means of some simple one-dimensional calculations using parameters for Armco iron. The model is strongly rate-dependent but time scales of a few microseconds are needed to resolve these rate effects. From the meager data available on geological materials, rate effects in rocks are believed to be of the same time scale. Since large-scale ground shock calculations are typically performed with time steps larger than 100 microseconds, it is impractical to consider using such a model for these problems and other modeling techniques should be considered.

Ultimately tensile failure always appears as a brittle phenomenon wherein a practically instantaneous stress drop occurs. In its idealized rate-independent form, brittle fracture is incompatible with stability and uniqueness theory for a continuum. (Once fracture occurs the material is no longer even a continuum.) However, two possible approaches should be examined since they may be acceptable for brittle tensile modeling in large-scale ground shock applications. Fortunately, these two approaches can be studied at the same time quite conveniently.

B. Recommendations

It is recommended that a series of one-dimensional problems be examined in order

(i) to determine if it is possible to use an idealized brittle fracture model in a wave code with the guarantee that a well-posed problem (with a unique solution) is being solved,

(ii) to test the range of validity of using a plasticity model in place of a brittle fracture model in ground shock applications.

One-dimensional wave propagation will be studied with a rate-independent brittle fracture model. This numerical model will be examined theoretically to try to determine if it represents a physically reasonable, mathematically well-posed problem. The plasticity model which is currently used in the cap model routine, Ref. [2], will also be used in the same wave code and the results will be examined with large-scale ground shock applications in mind. By this means it is hoped that an acceptable rate-independent tensile model can be developed.

REFERENCES

[1] Whitman, L. and Wright, J.P., 1975. "Tensile Behavior of Geological Material in Ground Shock Calculations", DNA 3769T, Weidlinger Associates, New York, N.Y.

[2] Sandler, I. and Rubin, D., 1975. "A Modular Subroutine for the Cap Model", DNA 3875F, Weidlinger Associates, New York, N.Y.

[3] Seaman, L., Barbee, T.W. and Curran, D.R., 1971. "Dynamic Fracture Criteria of Homogeneous Materials", Tech. Rep. No. AFWL-TR-71-156, Air Force Weapons Laboratory, Kirtland AFB, N.M.

[4] Seaman, L. and Shockey, D.A., 1973. "Models for Ductile and Brittle Fracture for Two-Dimensional Propagation Calculations", Final Report Draft, Contract No. DAAG46-72-C-0182, Army Materials and Mechanics Research Center, Watertown, Mass.

[5] Shockey, D.A., Seaman, L., Curran, D.R., DeCarli, P.S., Austin, M. and Wilhelm, J.P., 1973. "A Computational Model for Fragmentation of Armor Under Ballistic Impact", U.S. Army Ballistic Research Laboratories Report, Aberdeen Proving Ground, Md.

[6] Shockey, D.A., Petersen, C.F., Curran, D.R. and Rosenberg, J.T., 1973. "Failure of Rock Under High Rate Tensile Loads", New Horizons in Rock Mechanics, Fourteenth Symposium on Rock Mechanics, p. 709.

[7] Shockey, D.A., Curran, D.R., Seaman, L., Rosenberg, J.T. and Petersen, C.F., 1974. "Fragmentation of Rock Under Dynamic Loads", Int. J. Rock Mech. Sci. and Geomech. Abstr., 11, p. 303.

[8] Shockey, D.A., Curran, D.R., Austin, M. and Seaman, L., 1975. "Development of a Capability for Predicting Cratering and Fragmentation Behavior in Rock", DNA 3730F, Stanford Research Institute, Menlo Park, Calif.

[9] Carroll, M.M. and Holt, A.C., 1972. "Static and Dynamic Pore-Collapse Relations for Ductile Porous Materials", J. Appl. Phys., 43, No. 4, p. 1626.

[10] Sneddon, I.N. and Lowengrub, M., 1969. Crack Problems in the Classical Theory of Elasticity, John Wiley, New York.

[11] Shockey, D.A., Petersen, C.F., Curran, D.R., Rosenberg, J.T. and Seaman, L., 1973. "Dynamic Tensile Failure in Rocks", Final Report, Contract No. H0220053, U.S. Bureau of Mines, Twin Cities Mining Research Center, Twin Cities, Minn.

[12] Lawrence, R.J. and Mason, D.S., 1971. "WONDY IV - A Computer Program for One-Dimensional Wave Propagation with Rezoning", SC-RR-710284, Sandia Laboratories, Albuquerque, N.M.

[13] Jaeger, J.C. and Cook, N.G.W., 1969. Fundamentals of Rock Mechanics, Methuen, London.

[14] Al-Hussaini, M.M. and Townsend, F.C., 1974. "Investigation of Tensile Testing of Compacted Soils", S-74-10, U.S. Army Engineer Waterways Experiment Station, Vicksburg, Miss.

[15] Courant, R. and Hilbert, D., 1962. Methods of Mathematical Physics, Volume II, Partial Differential Equations, Interscience Publishers, John Wiley, New York.

[16] Maenchen, G. and Sack, S., 1964. "The Tensor Code", Methods in Computational Physics, Volume 3, Academic Press, New York.

[17] Burford, L., Thompson, J.C. and Cooper, Jr., H.F., 1971. "Spherical Wave Propagation in Brittle Materials", Dynamics of Rock Mechanics, Twelfth Symposium on Rock Dynamics.

DISTRIBUTION LIST

DEPARTMENT OF DEFENSE

Assistant to the Secretary of Defense
Atomic Energy
ATTN: Honorable Donald R. Cotter

Director
Defense Advanced Rsch. Proj. Agency
ATTN: STO
ATTN: NMRO
ATTN: PMO
ATTN: Tech. Lib.

Director
Defense Civil Preparedness Agency
Assistant Director for Research
ATTN: Admin. Officer

Defense Communications Agency
WWMCCS System Engineering Org.
ATTN: Thomas Neighbors

Defense Documentation Center
Cameron Station
12 cy ATTN: TC

Director
Defense Intelligence Agency
ATTN: DI-7E
ATTN: DB-4C, Edward O'Farrell

Director
Defense Nuclear Agency
ATTN: DDST
ATTN: TISI Archives
2 cy ATTN: SPSS
3 cy ATTN: TITL, Tech. Lib.

Chairman
Dept. of Defense Explo. Safety Board
ATTN: DD/S&SS

Commander, Field Command
Defense Nuclear Agency
ATTN: FCTMOF
ATTN: FCPR

Director
Interservice Nuclear Weapons School
ATTN: Doc. Con.

Director
Joint Strat. Tgt. Planning Staff, JCS
ATTN: STINFO Library

Chief
Livermore Division, Field Command, DNA
Lawrence Livermore Laboratory
ATTN: FCPRL

Under Secretary of Def. for Rsch. & Engrg.
ATTN: S&SS (OS)

DEPARTMENT OF THE ARMY

Director
BMD Advanced Tech. Ctr.
Huntsville Office
ATTN: CRDABH-S
ATTN: 1CRDABH-X

Dep. Chief of Staff for Rsch. Dev. & Acq.
ATTN: Tech. Lib.

Chief of Engineers
ATTN: DAEN-RDM
ATTN: DAEN-MCE-D

Dep. Chief of Staff for Ops. & Plans
ATTN: Tech. Lib.

Commander
Harry Diamond Laboratories
ATTN: DRXDO-TI, Tech. Lib.
ATTN: DELHD-NP

Commander
Redstone Scientific Information Ctr.
U.S. Army Missile Command
ATTN: Chief, Documents

Director
U.S. Army Ballistic Research Labs.
ATTN: Tech. Lib., Edward Baicy
ATTN: DRDAR-BLE, J. H. Keefer
ATTN: DRDAR-BLE, W. Taylor
ATTN: DRXBR-X, Julius J. Meszaros

Commander
U.S. Army Engineer Center
ATTN: ATSEN-SY-L

Division Engineer
U.S. Army Engineer Div., Huntsville
ATTN: HNDED-SR

Division Engineer
U.S. Army Engineer Div., Ohio River
ATTN: Tech. Lib.

Director
U.S. Army Engr. Waterways Exper. Sta.
ATTN: Guy Jackson
ATTN: John N. Strange
ATTN: Leo Ingram
ATTN: Tech. Lib.
ATTN: William Flathau

Commander
U.S. Army Mat. & Mechancis Rsch. Ctr.
ATTN: Tech. Lib.

Commander
U.S. Army Materiel Dev. & Readiness Cmd.
ATTN: Tech. Lib.

DEPARTMENT OF THE ARMY (Continued)

Commander
U.S. Army Nuclear Agency
ATTN: Tech. Lib.
ATTN: ATCA-NAW

DEPARMENT OF THE NAVY

Chief of Naval Material
ATTN: MAT 0323

Chief of Naval Operations
ATTN: Op-03EG
ATTN: Op-981

Chief of Naval Research
2 cy ATTN: Code 464, Thomas P. Quinn/Jacob L. Warner
ATTN: Nicholas Perrone
ATTN: Tech. Library

Officer-in-Charge
Civil Engineering Laboratory
Naval Construction Battalion Center
ATTN: Tech. Lib.
ATTN: Stan Takahashi
ATTN: R. J. Odello

Commander
Naval Electronic Systems Command
Naval Electronic Systems Cmd. Hqs.
ATTN: PME 117-21A

Commander
Naval Facilities Engineering Command
ATTN: Code 04B
ATTN: Code 03A
ATTN: Tech. Lib.

Superintendent (Code 1424)
Naval Postgraduate School
ATTN: Code 2124, Tech. Rpts. Librarian

Director
Naval Research Laboratory
ATTN: Code 2600, Tech. Lib.

Officer-in-Charge
Naval Surface Weapons Center
ATTN: Code WA501, Navy Nuc. Prgms. Off.

Commander
Naval Surface Weapons Center
Dahlgren Laboratory
ATTN: Tech. Lib.

Commanding Officer
Naval Underwater Systems Center
ATTN: Code EM, Jack Kalinowski

President
Naval War College
ATTN: Tech. Library

Commanding Officer
Naval Weapons Evaluation Facility
ATTN: Tech. Lib.

Director
Strategic Systems Project Office
ATTN: NSP-43, Tech. Lib.

DEPARTMENT OF THE AIR FORCE

AF Geophysics Laboratory, AFSC
ATTN: LWW, Ker C. Thompson
ATTN: SUOL, Rsch. Lib.

AF Institute of Technology, AU
ATTN: Library AFIT, Bldg. 640, Area B

AF Weapons Laboratory, AFSC
ATTN: DES-S, M. A. Plamondon
ATTN: SUL
ATTN: DES, G. Wayne Ullrich

Headquarters
Air Force Systems Command
ATTN: DLCAW

Commander
Foreign Technology Division, AFSC
ATTN: NICD Library

Hq. USAF/IN
ATTN: INATA

Hq. USAF/PR
ATTN: PRE

Hq. USAF/RD
ATTN; RDQSM

Commander Rome Air Development Center, AFSC
ATTN: EMTLD, Doc. Lib.

SAMSO/MN
ATTN: MNN

Commander in Chief
Strategic Air Command
ATTN: NRI, STINFO Lib.

DEPARTMENT OF ENERGY

Department of Energy
Albuquerque Operations Office
ATTN: Doc. Con. for Tech. Library

Department of Energy
Division of Headquarters Services
ATTN: Doc. Con. for Class. Tech. Lib.

Department of Energy
Nevada Operations Office
ATTN: Doc. Con. for Tech. Lib.

University of California
Lawrence Livermore Laboratory
ATTN: Larry W. Woodruff, L-96
ATTN: Tech. Info., Dept. L-3

Los Alamos Scientific Laboratory
ATTN: Doc. Con. for Reports Lib.
ATTN: Doc. Con. for R. J. Bridwell

Sandia Laboratories
Livermore Laboratory
ATTN: Doc. Con. for Tech. Library

Sandia Laboratories
ATTN: Doc. Con. for 3141, Sandia Rpt. Coll.
ATTN: L. Hill

DEPARTMENT OF ENERGY (Continued)

Union Carbide Corporation
Holifield National Laboratory
ATTN: Civil Def. Res. Proj.
ATTN: Doc. Con. for Tech. Lib.

OTHER GOVERNMENT AGENCY

Department of the Interior
Bureau of Mines
ATTN: Tech. Lib.

DEPARTMENT OF DEFENSE CONTRACTORS

Aerospace Corporation
ATTN: Tech. Info. Services

Agbabian Associates
ATTN: M. Agbabian

Applied Theory, Inc.
2 cy ATTN: John G. Trulio

Avco Research & Systems Group
ATTN: Research Lib., A830, Rm. 7201

Battelle Memorial Institute
ATTN: Tech. Lib.

The BDM Corporation
ATTN: Tech. Lib.

The Boeing Company
ATTN: Aerospace Library

California Research & Technology, Inc.
ATTN: Ken Kreyenhagen
ATTN: Tech. Lib.
ATTN: Sheldon Shuster

Calspan Corporation
ATTN: Tech. Lib.

Civil/Nuclear Systems Corp.
ATTN: Robert Crawford

University of Dayton
Industrial Security Super., KL-505
ATTN: Hallock F. Swift

University of Denver
Colorado Seminary
Denver Research Institute
ATTN: Sec. Officer for J. Wisotski

EG&G, Inc.
Albuquerque Division
ATTN: Tech. Lib.

Gard, Inc.
ATTN: G. L. Neidhardt

General Electric Company
TEMPO-Center for Advanced Studies
ATTN: DASIAC

IIT Research Institute
ATTN: R. E. Welch
ATTN: Milton R. Johnson
ATTN: Tech. Lib.

DEPARTMENT OF DEFENSE CONTRACTORS (Continued)

Institute for Defense Analyses
ATTN: IDA Librarian, Ruth S. Smith

Kaman AviDyne
Division of Kaman Sciences Corp.
ATTN: Tech. Lib.
ATTN: E. S. Criscione
ATTN: Norman P. Hobbs

Kaman Sciences Corporation
ATTN: Library

Lockheed Missiles & Space Co., Inc.
ATTN: Tech. Info. Ctr., D/Coll.
ATTN: Tom Geers, D/52-33, Bldg. 205

Lovelace Foundation for Medical
Education and Research
ATTN: Asst. Dir. of Res., Robert K. Jones
ATTN: Tech. Lib.

McDonnell Douglas Corporation
ATTN: Robert W. Halprin

Merritt CASES, Inc.
ATTN: J. L. Merritt
ATTN: Tech. Lib.

Nathan M. Newmark
Consulting Engineering Services
ATTN: Nathan M. Newmark

Physics International Company
ATTN: Doc. Con. for Tech. Lib.
ATTN: Doc. Con. for E. T. Moore
ATTN: Doc. Con. for Robert Swift
ATTN: Doc. Con. for Larry A. Behrmann
ATTN: Doc. Con. for Fred M. Sauer
ATTN: Doc. Con. for Dennis Orphal

R&D Associates
ATTN: Harold L. Brode
ATTN: Albert L. Latter
ATTN: Tech. Lib.
ATTN: Robert Port
ATTN: Henry Cooper
ATTN: Jerry Carpenter
ATTN: William B. Wright, Jr.
ATTN: J. G. Lewis

Science Applications, Inc.
ATTN: D. E. Maxwell
ATTN: David Bernstein

Science Applications, Inc.
ATTN: Tech. Lib.

Southwest Research Institute
ATTN: Wilfred E. Baker
ATTN: A. B. Wenzel

SRI International
ATTN: George R. Abrahamson
ATTN: Burt R. Gasten
ATTN: Y. Gupta

DEPARTMENT OF DEFENSE CONTRACTORS (Continued)

Systems, Science & Software, Inc.
ATTN: Tech. Lib.
ATTN: Donald R. Grine
ATTN: Ted Cherry
ATTN: Thomas D. Riney

Terra Tek, Inc.
ATTN: Tech. Lib.
ATTN: Sidney Green
ATTN: Ahmed Abou-Soyed

Tetra Tech., Inc.
ATTN: Li-San Hwang
ATTN: Tech. Lib.

TRW Defense & Space Sys. Group
ATTN: Tech. Info. Center, S-1930
ATTN: Pravin Bhutta, R1-1104
2 cy ATTN: Peter K. Dai, R1-2170

TRW Defense & Space Sys. Group
ATTN: E. Y. Wong, 527/712

Universal Analytics, Inc.
ATTN: E. I. Field

DEPARTMENT OF DEFENSE CONTRACTORS (Continued)

The Eric H. Wang
Civil Engineering Rsch. Fac.
ATTN: Neal Baum
ATTN: Larry Bickle

Weidlinger Assoc. Consulting Engineers
ATTN: Melvin L. Baron
ATTN: Joe Wright
ATTN: Lorraine Whitman

Weiglinger Assoc. Consulting Engineers
ATTN: J. Isenberg

Westinghouse Electric Corp.
Marine Division
ATTN: W. A. Volz